Appl. Phys. B 68, 735–739 (1999) / DOI 10.1007/s003409901400

Applied Physics B
Lasers
and Optics

Femtosecond nonresonant degenerate four-wave mixing at atmospheric pressure and in a free jet

H.-M. Frey, P. Beaud, T. Gerber, B. Mischler, P.P. Radi, A.P. Tzannis

Paul Scherrer Institute, General Energy Research, CH-5232 Villigen PSI, Switzerland
(Fax: +41-56/310-4416, E-mail: hans-martin.frey@psi.ch)

Received: 3 August 1998/Revised version: 21 October 1998/Published online: 24 February 1999

Abstract. Time-resolved nonresonant degenerate four-wave mixing (DFWM) experiments on the femtosecond time scale were performed in the gas phase. Results are presented for air, O_2, N_2, and CO_2. For CO_2 additional experiments have been performed at reduced pressure and in a molecular beam. By delaying the probe pulse a periodic recovery of the DFWM signal is observed. The period of these transients can be assigned unambiguously to rotational Raman transitions of the ground state within the laser bandwidth. The decay of the transients yields the collisional dephasing of the Raman-induced polarization. At zero delay also optical-field-induced birefringence of electronic nature contributes to the signal. The different time scales of the Raman and electronic effects allow us to estimate their relative strength.

PACS: 42.65.Dr

In the past years the application of fs lasers has gained major attention in both physics and chemistry. A variety of pump/probe techniques have been developed to obtain a deeper understanding of the dynamics in molecular systems [1]. In addition to methods with linear detection techniques such as resonant two-photon ionization and laser-induced fluorescence (for a full review see [2, 3]) the application of nonlinear techniques has been treated theoretically by Mukamel [4]. Recently, Motzkus et al. [5] used degenerate and two-color four-wave mixing to observe wave packet dynamics in molecular systems. Keiichi et al. [6] investigated the wavelength dependence of the Raman emission in hydrogen. Schmitt et al. [7, 8] reported on time-resolved coherent anti-Stokes Raman scattering (CARS) of iodine. They monitored the vibrational wave packet dynamics in iodine vapor. In contrast to other techniques the method is able to probe not only excited states but also the dynamics of the ground state. Besides vibrations, rotations can also be probed. Since the technique is sensitive to polarization the temporal response of coherently excited rotational states depends on their angular frequency. Analysis of the recurrences yields directly the moments of inertia and therefore for a known configuration, the structure of the molecule [9]. Rotational coherence of nitrogen, oxygen, and carbon dioxide has been investigated extensively by Morgen et al. [10] by fs Raman-induced polarization spectroscopy.

In this paper we report on fs DFWM experiments in air, O_2, N_2, and CO_2 yielding background-free, strong recurrence signals. A signal-to-noise ratio of 1000 is obtainable. The method has been applied in a cell at atmospheric pressure. To demonstrate its suitability for refined spectroscopic studies it was then successfully transferred into the collisionless environment of a molecular beam. The measurements were performed by operating the laser at a frequency far from any molecular resonance. It can be shown that the observed DFWM process originates from a third-order polarization, primarily induced by Raman transitions within the laser bandwidth. The rotational coherence of the Raman-induced polarization leads to sharp temporal recurrences of the DFWM signal when delaying the probe pulse with respect to the pump pulses. At time zero an additional nonresonant contribution to the DFWM signal due to the optical Kerr effect is observed. Besides the Raman effect already mentioned above, distortion of the electronic charge distribution, two-photon absorption, electrostriction, and molecular reorientation can also contribute to the optical Kerr effect [11]. However, the time scales involved in our experiment exclude effects from reorientation and electrostriction and limit our discussion to electronic distortion. From the transients of the Raman-induced polarization the rotational constants of the molecules can be extracted with good accuracy. The decay of the transients yields the collisional lifetime of the Raman-induced polarization. The beating between Stokes and anti-Stokes lines provides an estimate of the temperature of the molecules in the expansion zone of the molecular beam.

1 Experimental

Figure 1 shows the experimental setup. The laser source is an ultrashort Ti:sapphire laser system making use of the chirped pulse amplification technique (CPA 1000, Clark MXR, Dexter MI). The bandwidth-limited output pulses have a duration of 95 fs (assuming a Gaussian pulse shape) and a bandwidth

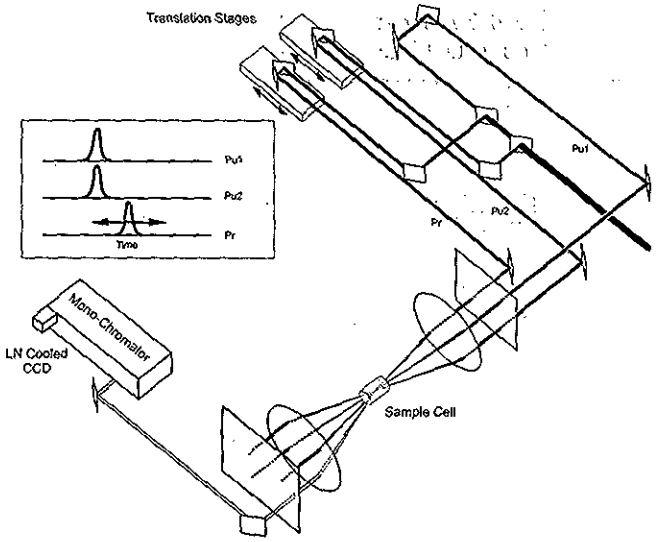

Fig. 1. Experimental setup. Pr: probe beam; Pu1&2: pump beams, all beams have the same intensity

of 9 nm. Except for the power dependence measurements the pulse energy is attenuated to 80 μJ/pulse at a repetition rate of 1 kHz. The laser wavelength is set to 795 nm. The beam is split into three equal parts, two pump beams (Pu1, Pu2) and one probe beam (Pr). The probe beam can be delayed with a computer-controlled translation stage (resolution of 0.3 μm or 3.33 fs). The three linear s-polarized beams are focused by a 500-mm lens into a cell (Suprasil, 100 mm) containing the sample gas at atmospheric pressure and room temperature. The cell could be alternatively replaced by a pulsed molecular beam (General Valve, backing pressure 2 bar (abs)). To maintain a reasonable pressure in the expansion chamber (10^{-4} mbar), the repetition rate of the system had to be reduced to 10 Hz. As in our previous work with ns resolution [12] the forward boxcar technique is used. The temporal and spatial overlap of the three pulses is optimized by second-harmonic generation in a 0.5-mm-thick BBO crystal. After recollimation the pump and probe pulses are blocked by a mask, and the signal is imaged onto the slit of a 500-mm monochromator. The DFWM signal is detected with a CCD or a photomultiplier. When not otherwise stated the spectrometer is used at total reflection in order to avoid spectral filtering of the DFWM signal.

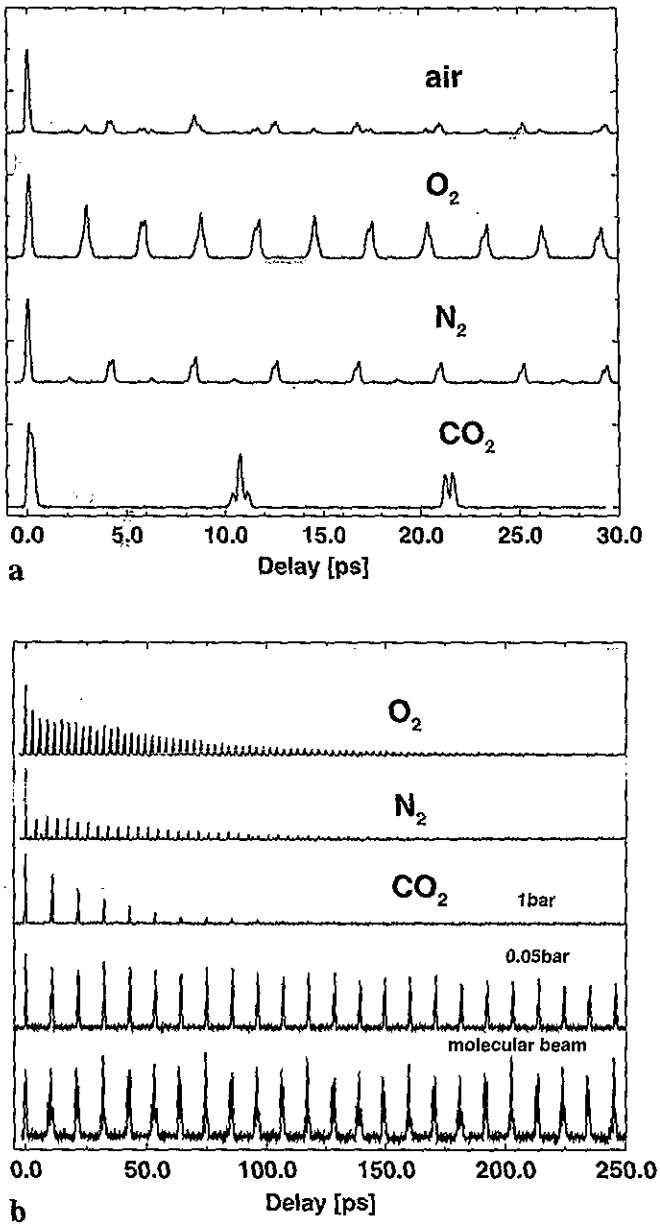

Fig. 2a,b. Short (a) and long range (b) DFWM transients of air, oxygen, nitrogen, and carbon dioxide

2 Results and discussion

With DFWM as a background-free technique a high signal-to-noise ratio is achieved. Figure 2a shows the DFWM signal in a cell experiment for time delays of the probe pulse up to 30 ps for air, O_2, N_2, and CO_2. Each molecule has its unique signature. The main features of the air transient can be attributed exclusively to its two major components N_2 and O_2. A contribution of CO_2 is not observed because of its rather low concentration in air of 0.03%. No saturation of the signals is observed for energy levels up to 110 μJ. Figure 3 shows the power dependence for oxygen in a logarithmic plot. As discussed later various effects contribute to the first signals in Fig. 2a. Despite this, both intensities at zero delay as well as the ones of subsequent recurrences show a third-order dependence indicating a pure $\chi^{(3)}$ process for all effects contributing to the signal.

The observed transients in the time domain may be explained as follows. Molecules excited via Raman transitions within the bandwidth of the pump pulses show an alignment in space according to their transition moment and the laser polarization. The orientation along the molecular axis for linear molecules that are marked with the two pump pulses will have a spatial distribution of $P(\Omega) = \cos^2(\Omega)$, with Ω being the angle between molecular axis (assuming transition moments parallel to the molecular axis) and the polarization vector. With time evolving, a molecule rotates out of its initial alignment and the signal eventually disappears. Recurrence of the original orientation will occur at $t = n/(2Bc\sqrt{J(J+1)})$ with n being an integer, J the rotational quantum number, B the rotational constant of the molecule in wavenumbers and

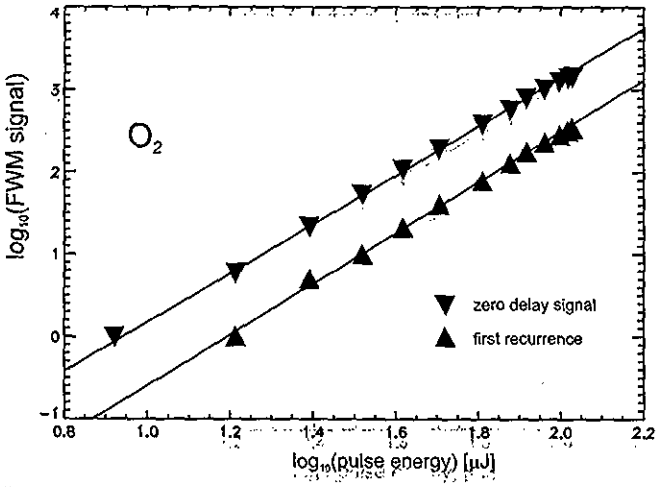

Fig. 3. Power dependence of the oxygen signal. Both the time zero signal and the first recurrence show a third-order dependence

c the speed of light. Taking into account the selection rules ($\Delta J = 0, \pm 2$) for Raman transitions and neglecting consequences of symmetry, the superposition of all signals having a cosine dependence will lead to sharp signals at multiples of the time $1/4Bc$.

Within the laser bandwidth of $140\,cm^{-1}$ we can only access rotational Raman transitions. Several third-order frequency arguments of the $\chi^{(3)}$ tensor based on the Raman effect are responsible for the observed signals. These are in particular the Raman-induced Kerr effect (RIKE), coherent anti-Stokes (CARS) and coherent Stokes Raman scattering (CSRS). Although the frequencies involved are not strictly degenerate, the phase mismatch for the Raman shifts observed ($< 100\,cm^{-1}$) is much smaller than that due to the divergence of the laser beam. Spatial filtering can therefore be neglected. The refracted probe beam still experiences a frequency shift corresponding to the Raman transition involved. Moreover, beating will occur between the spatially overlapping Stokes, anti-Stokes, and $\Delta J = 0$, frequencies.

A detailed interpretation of the observed transients can be achieved by Fourier analysis. For this purpose long transients covering a time delay up to 325 ps were recorded. The first 250 ps of the transients at atmospheric pressure is shown in Fig. 2b. Included are spectra of CO_2 taken at reduced pressure and in a molecular beam. Applying a FFT routine to these data results to the spectra shown in Fig. 4a. The frequencies of the first peak in the FFT spectra for O_2, N_2, and CO_2 are 11.482, 7.954, and $3.124\,cm^{-1}$, respectively. These frequencies can clearly be identified as the separation between successive rotational Raman transitions of the ground state of these molecules [13, 14]. For homonuclear molecules such as O_2 with a nuclear spin of 0 intercombination between symmetric and antisymmetric states is prohibited. Therefore, every second (the even ones in the case of O_2 having $^3\Sigma_g^-$ symmetry) transition is missing. The ground state of CO_2 ($^1\Sigma_g^+$) has a positive parity, therefore all levels with odd J are missing in the Raman spectrum. For N_2 with a nuclear spin of 1, we expect a 2:1 ratio in odd:even rotational bands. For O_2 and CO_2 the separation $\Delta\nu_R$ of successive Raman lines is $8B_0$, the ground state rotational constant and for nitrogen $\Delta\nu_R$ is $4B_0$ [13, 14]. Included in the spectrum are the different contributions from the beating in between the transitions $J = -2$, 0, and +2. All Fourier transforms show more than one sequence of equidistant lines. For the cell experiments with the molecules being at room temperature and at normal pressure, two sequences are observed. The first decays with increasing frequency. The second sequence has the same spacing, is shifted by half a period with respect to the power spectrum lines and reaches a maximum between 70 and $120\,cm^{-1}$ depending on the molecule. This modulation on the recurrences is due to the beating between Stokes $\leftrightarrow$ anti-Stokes polarization. Since for O_2 and CO_2 the lowest Raman transition is $5\Delta\nu_R/4$, the beating between Stokes and anti-Stokes signals can be observed in the FFT spectra as lines at $(n + 5/2)\Delta\nu_R$ with n being a positive integer. For N_2 these corresponding lines are found at $(n+3)\Delta\nu_R$. For further evidence we recorded DFWM transients with the spectrometer set at the wings of the signal spectrum (either to the Stokes or anti-

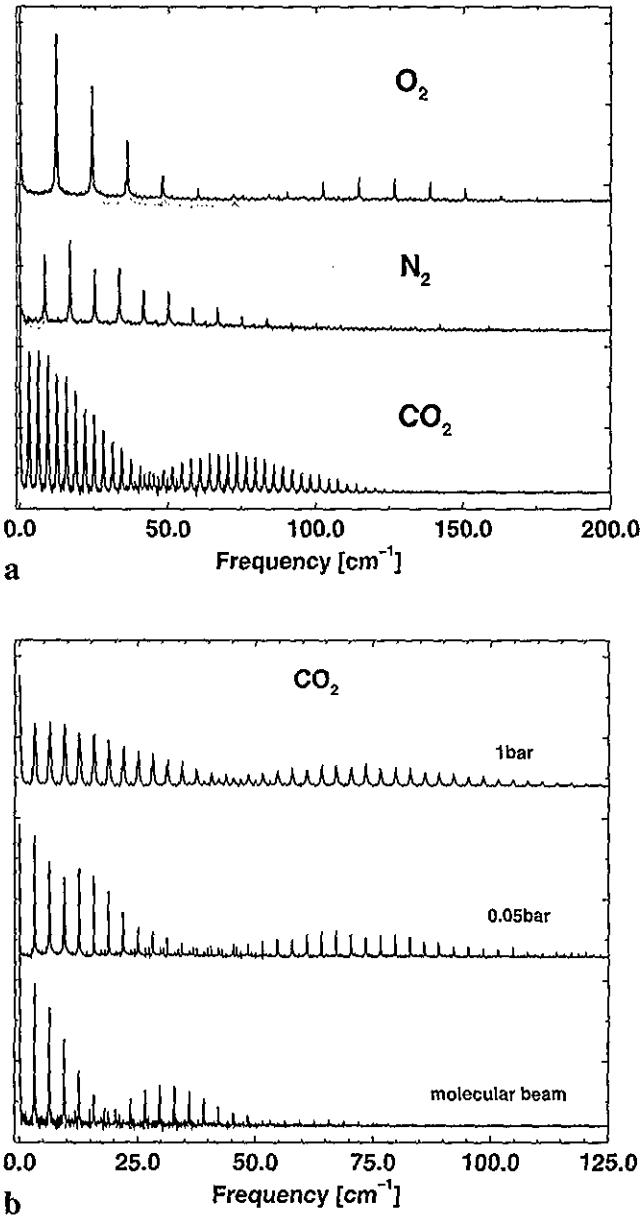

Fig. 4. Fourier transform spectra of oxygen, nitrogen, and carbon dioxide. The spectra are the discrete transforms of the transients in Fig. 2b

Stokes side). As expected the modulations disappear yielding sharp unmodulated recurrence peaks. In the cell experiment at reduced pressure and in the molecular beam experiment additional beating with a maximum at 30 cm^{-1} can be extracted (Fig. 4b). The shift of the peaks of 1/4 line separation in relation to the main sequence indicates an origin that arises from the beating between Stokes or anti-Stokes with the transition $\Delta J = 0$. The shape of both beating sequences depends on the rotational distribution and therefore of the temperature of the molecule. In Fig. 5 temperature simulations are included in the FFT spectrum for CO_2 in the molecular beam. The values are obtained assuming a Boltzmann distribution and neglecting the dependence of the Raman transition probabilities to the rotational excitation J. Simulations are shown for $T = 50$, 100, and 150 K for the Stokes $\leftrightarrow$ anti-Stokes beating sequence. For the beating Stokes $\leftrightarrow \Delta J = 0$ only the matching fit of $T = 100$ K is included. The value of 100 K obtained by fitting is in accordance with expectations of a unseeded molecular beam close to the nozzle. The experiments at room temperature (atmospheric and reduced pressure) yield an estimate that is too high. At low J the collisional energy transfer is more probable than for high J [15]. As a consequence, collisional dephasing is stronger for low J, yielding an apparent higher temperature.

The values for B_0 derived from our experiment are summarized in Table 1 and compared to published values [13, 14]. Within the experimental uncertainty good agreement is found.The results are obtained using the fundamental frequency $\Delta\nu_R$ of the measured rotational recurrences only. It is important to emphasize that the rotational, as well as the centrifugal and spin–spin splitting constants can be obtained with much higher precision when fitting a nonrigid rotor to the measured transients [16]. Such a detailed analysis, however, would go beyond the scope of the present study.

Table 1. Molecular constants (rotational and collisional) extracted from fs DFWM experiment, and relative strength of electronic and Raman effects

	B_0 /cm^{-1} experiment	B_0 /cm^{-1} literature [11, 12]	τ /ps	$\chi_R^{(3)}/\chi_{NR}^{(3)}$
O_2	1.435 ± 0.013	1.438	68	≈ 2
N_2	1.989 ± 0.026	2.007	61	≈ 1
CO_2	0.390 ± 0.013	0.390	30	$\gg 1$

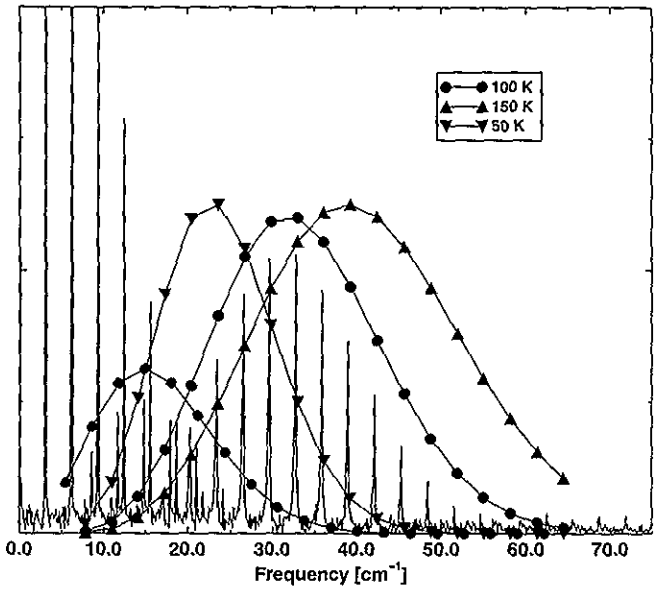

Fig. 5. Temperature estimate for a pure CO_2 expansion. For the most probable temperature of 100 K the shapes of the beating of $\Delta J = 0$ with $\Delta J = \pm 2$ (peak at 15 cm^{-1}) and the $J = -2$ with $J = 2$ (peak at 33 cm^{-1}) are plotted

The decay of the transients as shown in Fig. 2b yields the collisional lifetime of the Raman-induced polarization. In Fig. 6 the peak integrals of the individual recurrences are plotted on a logarithmic scale versus time. The fitted slopes are related to the collisional cross sections for O_2–O_2, N_2–N_2, and CO_2–CO_2 collisions in the ground states of these molecules for atmospheric pressure and room temperature. The corresponding lifetimes τ are included in Table 1. Since the signals are normalized at $t = 0$, the fitted curves must cut the origin of Fig. 6 if no other effect contributes to the DFWM signal. As seen in Fig. 6 this is the case for carbon dioxide only. For oxygen and nitrogen the Raman process contributes only approximately 2/3 and 1/2, respectively, to the DFWM signal measured at time zero. For the peaks at $t = 0$ an additional contribution by another effect has to be considered. Since the additional signal is observed only during the temporal overlap of all three input pulses the response time of this process must be shorter than the laser pulse, i.e., less than 100 fs, the temporal resolution of our experiment. Of the additional processes that contribute to the optical Kerr effect (see above) only field-induced distortion of the electronic charge distribution is fast enough. Far from any resonance of the media this process has a response time on the order of 1 fs [17]. Other possible effects are either much slower (electrostriction and molecular reorientation) or nonexistent at our laser frequency (two-photon transitions). The resulting ratios $\chi_R^{(3)}/\chi_{NR}^{(3)}$ of the resonant (Raman) and nonresonant (electronic) contribution to the induced third-order polarization are shown in Table 1. The Raman term depends on the number of available transitions within the laser bandwidth and on the population of the participating rotational states. Consequently, the ratio $\chi_R^{(3)}/\chi_{NR}^{(3)}$ depends on the tempera-

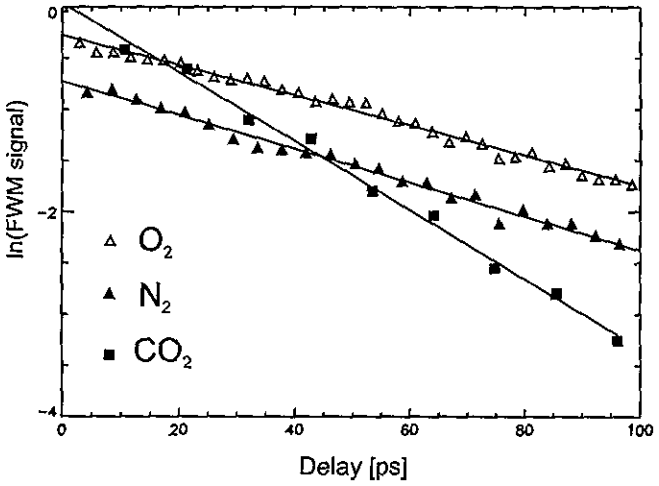

Fig. 6. Strength of the individual recurrence peaks versus time delay of the probe pulse on a logarithmic scale

ture and on the bandwidth of the laser pulses. Our experiment shows that $\chi_{NR}^{(3)}$ and $\chi_{R}^{(3)}$ are on the same order of magnitude for O_2 and N_2 and $\chi_{NR}^{(3)}$ is negligible for CO_2.

3 Conclusion

We have shown that fs DFWM is applicable for spectroscopy of the ground state even though the laser frequency is chosen far from any electronic resonance. The signal intensities are sufficient to obtain spectra in a pulsed molecular beam with a sufficient signal-to-noise ratio. The Raman-induced polarization leads to rotational recurrences of the signal from which the rotational constants of the molecules can be extracted. The decay of the transient yields the collisional dephasing of the Raman-induced polarization depending on the pressure. At zero delay optical-field-induced birefringence of electronic nature also contributes to the signal. The different temporal evolution of the Raman and electronic contributions to the third-order polarization allows us to estimate their relative strength. Besides its capability to investigate rotational relaxation in the ground state the technique can also be applied as an analytical tool to detect species with a known rotational constant.

Acknowledgements. This work was supported by the Swiss Department of Energy (BEW).

References

1. S. Pedersen, A.H. Zewail: Mol. Phys. **89**, 1455 (1996)
2. A.H. Zewail: *Femtochemistry-Ultrafast Dynamics of the Chemical Bond* (World Scientific, Singapore 1994)
3. J. Manz, L. Wöste: *Femtosecond Chemistry* (VCH, Weinheim 1995)
4. S. Mukamel: *Nonlinear Optical Spectroscopy* (Oxford University Press, Oxford 1995)
5. M. Motzkus, S. Pedersen, A.H. Zewail: J. Phys. Chem. **100**, 5260 (1996)
6. O. Keiichi, K. Hiroyuki, H. Yasuyuki, I. Totaro: Jpn. J. Appl. Phys. **36**, 6376 (1997)
7. M. Schmitt, G. Knopp, A. Materny, W. Kiefer: Chem. Phys. Lett. **270**, 9 (1997)
8. M. Schmitt, G. Knopp, A. Materny, W. Kiefer: J. Phys. Chem. A **102**, 4059 (1998)
9. J.S. Baskin, P.M. Felker, A.H. Zewail: J. Chem. Phys. **84**, 4708 (1986)
10. M. Morgen, W. Price, L. Hunziker, P. Ludowise, M. Blackwell, Y. Chen: Chem. Phys. Lett. **209**, 1 (1993)
11. Y.R. Shen: *The Principles of Nonlinear Optics* (Wiley, New York 1984)
12. P.P. Radi, H.M. Frey, B. Mischler, A.P. Tzannis, P. Beaud, T. Gerber: Chem. Phys. Lett. **265**, 271 (1997)
13. G. Herzberg: *Spectra of Diatomic Molecules* (Robert Krieger, Malabar, Florida 1950)
14. G. Herzberg: *Electronic Spectra of Polyatomic Molecules* (Van Nostrand Reinhold Company, New York 1966)
15. P. Beaud, P.P. Radi, D. Franzke, H.-M. Frey, B. Mischler, A.P. Tzannis, T. Gerber: App. Opt. **37**, 3354 (1998)
16. M. Morgen, W. Price, P. Ludowise, Y. Chen: J. Chem. Phys. **102**, 8780 (1995)
17. P.N. Butcher, D. Cotter: *The Elements of Nonlinear Optics* (Cambridge University Press, Cambridge 1990)